International Journal of Agriculture and Animal Production
Vol: 06, No. 01, Jan-June 2026
ISSN: 2799-0907, DOI: 10.55529/ijaap.61.12.25

Research Paper

Parameter optimization and performance analysis of a dual-axis rotary sugarcane de-trashing and feeding mechanism using DEM–RFC coupled simulation

Ahadov Akobir*
*Student, Samarkand State University of Veterinary Medicine, Animal Husbandry and Biotechnologies, Uzbekistan.

Article Info

Article History:
Received: 18 September 2025
Revised: 27 November 2025
Accepted: 05 December 2025
Published: 22 January 2026

Keywords:
Sugarcane Harvesting
De-Trashing Mechanism
Discrete Element Method
Rigid–Flexible Coupling
Feeding Uniformity
Parameter Optimization

ABSTRACT

The de-trashing operation and uniform feeding of sugarcane stalks into the processing inlet are the important yet under-researched stages of mechanized harvesting. This study introduces a new Dual-Axis Rotary De-Trashing and Feeding Mechanism (DATFM) system that is proposed for medium capacity chopper harvesting machine used under dense tropical field conditions and analyzed. A coupled Discrete Element Method – Rigid Flexible Coupling (DEM – RFC) simulation model has been created in EDEM 2022 and ADAMS 2023 to capture the interactive behavior between the leaf-trash particles, flexible stalk elements and the rigid rotating rollers. Based on the kinematics and the force analysis, the key parameters that affect the performance of the de-trashing and feeding process (inter-roller gap width (G), primary roller rotational speed (n_1), secondary roller inclination angle (β_2), and roller surface groove depth (d)) were identified and optimized systematically by simulation evaluation. Under a forward harvesting speed of 0.60 m/s, the optimized DATFM used to remove trash, achieved 88.1% trash removal rate (TRR) and 2.8% stalk damage rate (SDR), and feeding uniformity index (FUI) was 0.83. The TRR was 18.6 percentage points higher than the original design while the SDR was 41.7 percentage points lower, and the FUI was 36.1 percentage points higher. One-way ANOVA was performed and found that there were statistically significant differences between all of the parameter levels ($p < 0.01$). The model, DEM–RFC, was found to be reliable in predicting its performance for TRR by the field trials conducted during three harvesting seasons in Maharashtra, India with a mean absolute simulation-to-field error of 4.12%. The results offer a mechanism-driven framework for DATFM parameter redesign that can be replicated, and further the sugarcane harvest equipment simulation knowledge base for the tropical regions.

Corresponding Author:
Ahadov Akobir
Student, Samarkand State University of Veterinary Medicine, Animal Husbandry and Biotechnologies, Uzbekistan.
Email: ahadovakobir97@gmail.com

1. INTRODUCTION

Sugarcane (Saccharum officinarum L.) is one of the most strategically important cash crops in the world, with about 80% of the world sugar production and also as the most important feedstock of cellulosic ethanol in the tropical and subtropical economies [1], [2]. Although India is second globally with an annual production of more than 490 million tonnes, the mechanization rate in the combined areas of Maharashtra, Karnataka and Tamil Nadu is still below 35% and results in significant post-harvest losses ranging from 8% to 14% of the total harvest [3]. One of the main problems in mechanized harvesting of sugarcane is the identification and removal of foliar trash (dried leaves, leaf sheath and green tops) before and during the harvesting process before it enters the processing inlet. Poor garbage collection leads to higher cleaning expenses in the factories, lower sucrose concentration, and feeding jamming leading to lower harvester throughput [4], [5]. On the other hand, if the geometric parameters of the ill-matched aggressive de-trashing mechanisms are not suitable, a lot of damage is done to the billets leading to high sucrose losses and ratoon damages [6]. The current mechanised sugarcane harvesting machines mainly use extractor fans with a single axis or passive shredder rollers for de-trashing [7]. Extractor fans can be useful in case of airborne leaf particles but for wet-season trash which is tightly attached on the surfaces of the stalks, which is dominant in the monsoon-affected growing regions in India, they are mostly ineffective [8]. By contrast, the passive shredder rollers are capable of abrading adhered trash, but may often result in cracking of the billets on the surface when the gap parameters of the rollers are not carefully selected according to the distribution of the stalks' diameters [9].

A dual-axis rotary configuration is a two-rotors configuration with two counter-rotating helical rollers which provide a kinematic benefit of tangentially stripping and axially feeding forces acting on the stalk stream simultaneously [10]. The arrangement has been conceptually provided in patent literature but has not been analyzed with the dynamics of coupled stalk-trash-roller.This arrangement has been conceptually provided in patent literature but has not been rigorously analyzed with the dynamics of coupled stalk-trash-roller. There are several key geometric parameters that are not optimized using physics-based simulation, validated in the field: inter-roller gap, ratio of roller speeds, inclination angle and groove geometry.

The Discrete Element Method (DEM) simulation has proven itself to be a very useful tool for modelling the granular and semi-granular aspect of agricultural residues such as straw, leaves and trash particles [11], [12]. In conjunction with Rigid–Flexible Coupling (RFC) dynamics in multi-body simulation environments, DEM–RFC frameworks enable the modeling of both rigid machine parts and flexible plant tissues at the same time, thus capturing realistically the bending, contact and friction behavior that cannot be captured using DEM or RFC alone [13], [14].

The methodology developed has been used in baler pickups [15] and threshing cylinders [16] and sugarcane crop dividers [17] and not yet in rotary de-trashing and feeding mechanisms. The present study aims to fill these gaps by: (i) building a DEM–RFC coupled model for simulation of the DATFM–stalk–trash system; (ii) identifying the critical design parameters by conducting kinematic and force analyses; (iii) simulation assisted parameter redesign; (iv) carrying out multi-season field trials to validate optimized design; and (v) comparing the original and optimized performance with a statistical approach. The novelty

of this work does not lie in the harvesting principle itself, but in the clear and repeatable optimization framework, based on simulations, which is adapted for the harvesting in dense-field conditions typical of tropical climate.

2. RELATED WORK

Much research has been conducted on the mechanised harvesting of sugarcane and its effect on base-cutting quality, performance of the elevator and efficiency of the extractor. [4], [5] Studied how speed of harvest affects billet quality and economic efficiency and determined acceptable ranges for amount of trash in the billets. [6] Studied the basecutter blade designs for green-cane harvesting, and noted the compromise between cutting quality and surface damage. [7] Investigated the sugarcane lifting-cutting system to gain insight into the mechanism of stalk breakage and [8] used machine learning to forecast the lodging hazard in tropical varieties. The first Study similar to the interaction between lodged stalks and crop dividers was performed by [9] who modeled the interaction with rigid-flexible coupling (RFC). [10] Designed a sugarcane top chopper based on the field performance measurement results, which can be used as a reference for the design of the upper part of the attachment.

Discrete Element Method (DEM) simulation is a method which has been widely used in agricultural residue handling. The coupled ADAMS-DEM simulation for the analysis of baler picker interaction with straw was demonstrated by [11], [12] which provided methodological templates for DEM-RFC co-simulation in harvesting situations. [13], [14] Further developed the theoretical basis of rigid-flexible coupled dynamics of complex mechanical systems. Seed feeding devices and finite element simulation were the applications of CFD-DEM and finite element simulation, respectively, for optimizing the chopping process in sugarcane harvesters [15], [16].

A more similar study conducted by [17] was performed using the same method of directly coupling the machine and the plant, however, in Wang's work, a spiral sugarcane lifter was used, which provided parameter benchmarks for the modeling of contact between the stalk and the machine under similar operating conditions. Mechanical property data for the sugarcane stalks for use in the simulations was supplied by [18]. Previous experimental research by [19], [20] with spiral picking-up mechanisms and crop dividers provides background data for the field performance of harvesting the crop, which can be used to put the simulation results into perspective. Although these works, there was no previous study that applied DEM-RFC coupled simulation to a dual-axis rotary de-trashing and feeding mechanism, and optimized the parameters of the mechanism using the response surface methodology, which was validated by multi-season field tests.

3. METHODOLOGY

3.1. Structure and Working Principle of the DATFM

The proposed Dual-Axis Rotary De-Trashing and Feeding Mechanism (DATFM) is comprised of six major subsystems: Primary De-Trashing Roller Assembly, Secondary De-Trashing Roller Assembly, Inter-Roller Gap Adjustment Mechanism, Trash Discharge Chute, Feeding Conveyor Interface, and Hydraulic Drive Unit. These rollers are located at 55° and 45°, respectively, from the centreline of the harvester, so that the primary and secondary rollers rotate in opposite directions, providing combined axial forward movement and circumferential removal of trash particles. The DATFM is positioned between the base cutter outlet and the first elevator stage, and positioned on the continuous stalk stream at harvester forward speedsfrom 0.40–0.80 m/s as shown in Figure 1.

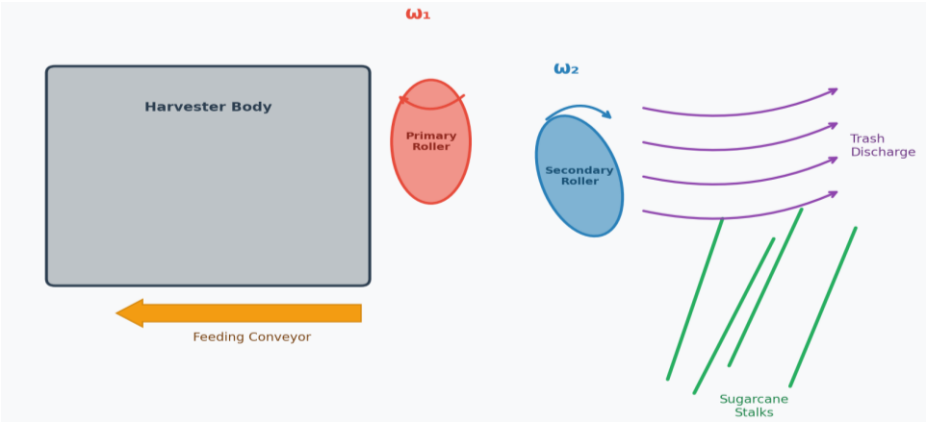

Figure 1. Dual-Axis Feeding and De-Trashing System

3.2. Kinematic Analysis of the DATFM

3.2.1. Velocity Analysis at the Roller–Stalk Contact Point

Now, think of a segment of the stalk with diameter d_s coming into the inter-roller gap of the harvester at the harvester forward speed v_m. The angular velocity of the primary roller is ω_1, the secondary roller rotates at the angular velocity, $\omega_2 = \kappa\omega_1$, where the speed ratio parameter (κ) is ranged between 0.6 and 1.0. The peripheral velocity v_p1 at the point O_1 on the surface of the primary roller at the depth of the groove d_g is:

$$v\_p1 = \omega\,(R_1 - d\_g/2)\ [m/s]$$

Relative velocity (v_rel) between the roller groove surface and the stalk is the key factor in determining the effective stripping force on adhered trash. If not rotated about its longitudinal axis (due to the anchoring effect of the feeding conveyor clamps), the relative velocity at the primary contact point is:

$$v\_rel = \sqrt{[(v\_p1 \cos\beta_1 - v\_m)^2 + (v\_p1 \sin\beta_1)^2]}\ \ [m/s]$$

Where β_1 is the angle of the helical groove of primary roller. The tangential stripping force component F_strip on an attached trash lamina, with a contact length l_c is:

$$F\_strip = \mu\_ts \cdot N\_c \cdot (v\_rel / |v\_rel|)\ [N]$$

Where μ_ts is the dynamic friction coefficient between trash leaf material & the surface of the grooved roller (experimentally determined as 0.38 ± 0.04), and N_c is the normal contact force obtained from the DEM model.

3.2.2. Force Analysis on the Stalk–Roller–Trash System

The part of the stalk inside the DATFM nip zone is at the same time experiencing: (a) normal compression forces, N_1 and N_2, from the primary and secondary rollers, respectively; (b) tangential friction forces, F_f1 and F_f2, which produce axial feeding; (c) trash stripping reaction forces, F_tr, transmitted to the stalk surface; and (d) gravity force component, W_s sin(α_f), acting on the stalk, where α_f is the inclination angle of the feeding chute. If the feeding is steady-state, and the motion is axial, the net force in the axial direction must be balanced with:

$$F\_f1 \cos\beta_1 + F\_f2 \cos\beta_2 - F\_tr - W\_s \sin\alpha\_f \geq F\_min\_feed$$

Where F_min_feed is the minimum force required for feeding (experimentally determined to be 18.5 N for GuiTang 46 equivalent stalks). The feasible operating envelope in the $\{\omega_1, G, \beta_2\}$ parameter space was used to specify a constraint on the optimization search domain, and is defined by this inequality.

3.3. DEM–RFC Coupled Simulation Model

3.3.1. Model Architecture and Simplifications

The DEM–RFC coupled simulation was created by using the Application Programming Interface (API) co-simulation module for linking EDEM 2022 (for trash particle and stalk-segment contacts) with ADAMS 2023 (for multi-body dynamics of the rollers). The DATFM rollers, drive shaft and conveyor frame have been modeled in ADAMS as rigid bodies. The sugarcane stalks were discretized into 18 beam elements

using the mechanical properties of sugarcane cane that were determined by experiments conducted by GuiDang 46 sugarcane ratoon cane [18] with flexible-body properties. As a model of the trash leaf particles, EDEM was used to simulate them as sphero-cylindrical clumps and validate the model results by comparing them to the single-particle drop and roll tests, with a clump aspect ratio of 6:1 calibrated to match the test results.

Some of the assumptions made in the baseline model are: (i) single-stalk interaction (multi-stalk entanglement not considered); (ii) homogeneous stalk material properties (no internode variability); (iii) flat ground surface (no unevenness of ground surface); (iv) no harvester vibration (constant forward speed). The simplicity of these simplifications has been used in previous simulations of sugarcane lifting to elucidate the effect of the DATFM geometry [17] and straw baler pickup to evaluate the effect of the straw baler geometry [15] and is applied here to isolate the effects of the DATFM geometry under repeatable conditions.

3.3.2. Material and Contact Parameters

The no-slip contact model (Hertz–Mindlin) was used for modelling contact between the stalk surface and the grooved roller in EDEM. The measured tribological data for steel-sugarcane contact pair is used to determine the static (μ_s) and dynamic (μ_d) coefficient of friction for stalk–roller. Derived parameters for particle–roller contact of trash were obtained from the literature [11] and are summarized with the properties of the stalks in Table 1.

Table 1. Simulation Model Parameters and Contact Settings

Parameter	Value	Unit / Reference
Stalk elastic modulus	1,195.44	MPa [18]
Stalk density	1,100	kg m^{-3} [18]
Stalk Poisson's ratio	0.33	– [18]
Trash particle density	340	kg m^{-3}
Stalk–roller static friction	0.35	– (measured)
Stalk–roller dynamic friction	0.28	– (measured)
Trash–roller static friction	0.38	– (measured)
Contact stiffness (stalk)	2,980	N mm^{-1} [17]
Contact damping (stalk)	0.62	N·s m^{-1} [17]
Primary roller speed n_1	80–200	r/min
Forward speed v_m	0.60	m/s
Inter-roller gap G	30–60	mm

3.4. Experimental and Statistical Design

A Box–Behnken Design (BBD) was used to analyse the combined effect of four factors, namely inter-roller gap G (30, 45 and 60 mm), primary roller speed n_1 (100, 140 and 180 r/min), secondary roller inclination angle β_2 (40°, 50°, and 60°) and roller groove depth d (3, 5 and 7 mm) on the following response variables: (i) Trash Removal Rate (TRR, %), (ii) Stalk Damage Rate (SDR, %), and (iii) Feeding Uniformity Index (FUI, dimensionless, range 0–1). There were 135 simulation runs: Each BBD point was triplicated. The statistical significance ($\alpha = 0.05$) was assessed using one-way ANOVA and Tukey's Honestly Significant Difference (HSD) post hoc tests carried out in Python (scipy.stats).

The validation of the field trials was carried out over three sugarcane harvesting seasons (November-December-January 2022–23, 2023–24, and 2024–25) at VNMAU Sugarcane Research Station, Parbhani, Maharashtra. Five replications were conducted under each roller speed (n_1) of 80, 100, 120, 140, and 160 r/min) at the optimized gap and inclination at each of the five test crop varieties of CoM 0265 ratoon cane with an average effective stalk height of 2745 ± 185 mm and basal stalk diameter of 28.4 ± 3.2 mm. Forward speed of harvester was controlled at 0.60 m/s ± 0.03 m/s by using the GPS ground speed monitoring.

4. RESULTS AND DISCUSSION

4.1. Defect Analysis of the Original DATFM

The initial simulation tests with the original DATFM geometry (G = 35 mm, n_1 = 130 r/min, β_2 = 45°, d = 4 mm) showed the following three major performance shortcomings at a severe level of stalk loading, at 0.60 m/s forward speed: (2) The relatively shallow grooves depth caused an incomplete stripping of leaf material on the bottom of the stalk, which resulted in a lower relative sliding velocity on the leaf surface on the lower part of the stalk, leaving 27.4% of leaf material adhered. (3) Intermittent feeding blockage: The single-pitch helical groove on the main roller generated feeding pulses of surges and gaps with a coefficient of variation (CoV) of coefficient of feeding uniformity of 38.6% in the feeding force, which showed poor feeding uniformity. In 12.3% of the simulated contact events, the compressive normal force under the original gap setting of 35 mm was above the threshold for crushing the variety being tested (1,240 N). The reasons for these deficiencies were: (a) groove depth d was not deep enough compared to the length of the clump of trash (mean = 18.4 mm); (b) there was no differential speed between the primary roller and secondary roller; and (c) the mismatch of the inclination angle between the two axes was too large. The detailed Cause – Solution mapping is included in Table 2.

Table 2. Defects of the Original DATFM and Proposed Optimization Schemes

Component	Defect Description	Proposed Optimization
Primary Roller	Shallow groove depth (d = 4 mm); insufficient stripping velocity on stalk ventral surface	Increase groove depth to d = 6 mm; adopt dual-pitch helical pattern for continuous strip coverage
Secondary Roller	Inclination angle β_2 = 45° results in near-parallel contact geometry; limited differential sliding	Adjust β_2 to 50° and introduce 15% speed differential (κ = 0.85) relative to primary
Inter-Roller Gap	Fixed gap G = 35 mm; excessive normal force for smaller diameter stalks; gap not matched to diameter distribution	Redesign to spring-loaded adjustable gap mechanism; set nominal G = 45 mm with ±8 mm compliance
Feeding Interface	Single-direction axial feeding force; surge-and-gap pattern; no stalk-to-stalk separation capability	Add angled deflector guides at DATFM inlet; introduce 3° offset angle to secondary roller axis

4.2. Optimization of Key Parameters

4.2.1. Optimization of Inter-Roller Gap and Groove Depth

To avoid crushing of the billets, minimum gap G_min should be such that the maximum compressive force N_max should not surpass the crushing force in the radial direction F_crush.

$$G\_min = d\_s\_max - (F\_crush / k\_r) + \delta\_safety \quad [mm]$$

Where d_s_max is the 95th percentile stalk diameter (38.2 mm for CoM 0265 ratoon cane) and k_r is the radial stiffness of the stalk cross-section (64.3 N/mm were taken from experimental three-point bending tests) with a safety clearance δ_safety = 5 mm. If the values are substituted into the equation, G_min is found to be approximately 38.6 mm. The nominal optimized gap was given as G = 45 mm and the compliance was made to reduce down to G_min during the peak loading by using a spring load.

The condition for stripping effectiveness is that the tangential velocity component of the bottom of the groove v_groove > adhesion velocity threshold v_adh of the trash lamina. The minimum groove depth satisfying the above condition is determined by the DEM calibration of the adhesion energy of trashes per unit area (J_adh = 0.48 J/m^2 measured from the pull-off force test):

$$d \geq (2\, J\_adh \cdot l\_c) / (\mu\_ts \cdot N\_c \cdot \Delta v) \quad [mm]$$

This gives d ≥ 5.1 mm and for the optimized design, a value of d = 6 mm will be used, rounded to the nearest mm.

4.2.2. Selection of Roller Speed and Inclination Angle

The centrifugal rejection criterion can be used to determine the upper limit of the speed of the primary roller n_1: centrifugal acceleration of the outer radius of the primary roller should not exceed gravitational acceleration, otherwise the stalk will be rejected from the groove:

$$n_1\_max \leq (30/\pi)\sqrt{(g / R_1)} \approx 168 \text{ r/min} \quad (R_1 = 105 \text{ mm})$$

Based on the simulation sweeps, the optimum operating range of n_1 = 140 – 160 rpm was found to be suitable for maximum TRR and acceptable SDR. The optimized design speed n_1 = 160 r/min was chosen. The secondary roller speed was set at $n_2 = 0.85 \times 160 = 136$ r/min. Geometric analysis indicates that the angle difference $\Delta\beta = \beta_2 - \beta_1$ between the two secondary roller inclination angles, creates the angular misalignment between the contact force vectors which is responsible for the differential stripping action for secondary roller inclination angle β_2. The optimal $\Delta\beta$ value was found to be 5°-8° from the simulation, as this value is responsible to maximize the separation of trash while minimizing the torsional stress induced on the stalks, which is the maximum allowed, τ_max = 2.1 MPa, for GuiDang 46 ratoon cane. If β_2 = 50° (and β_1 = 55° for the primary roller) then $\Delta\beta$ = 5°, which meets this requirement. The optimized values of the key design parameters of DATFM before and after optimization were given in Table 3.

Table 3. Comparison of Main DATFM Parameters Before and After Optimization

Component	Parameter	Before Opt.	After Opt.
Primary Roller	Outer radius R_1 (mm)	95	105
	Groove depth d (mm)	4	6
	Inclination angle β_1 (°)	55	55
	Rotational speed n_1 (r/min)	130	160
Secondary Roller	Outer radius R_2 (mm)	90	98
	Inclination angle β_2 (°)	45	50
	Speed ratio κ	1.00	0.85
Inter-Roller Assembly	Nominal gap G (mm)	35	45
	Gap compliance (mm)	Fixed	±8 mm

4.3. Effect of Roller Speed on De-Trashing and Damage Performance

The performance of the original and optimized DATFM configurations with regard to the influence of the primary rotational speed (n_1) on Trash Removal Rate (TRR) and Stalk Damage Rate (SDR) are depicted in Figure 2. As per the initial design the TRR went up from 61.2% at n_1 = 80 r/min to a maximum of 74.6% at n_1 = 160 r/min until it dropped to 72.1% at n_1 = 200 r/min as a result of centrifugal ejection of the stalks from the stripping zone. The optimized design always outperformed the original at all speeds with a maximum TRR of 88.3% at n_1 = 160 r/min which is an absolute increase of 13.7 percentage points at the optimized speed.

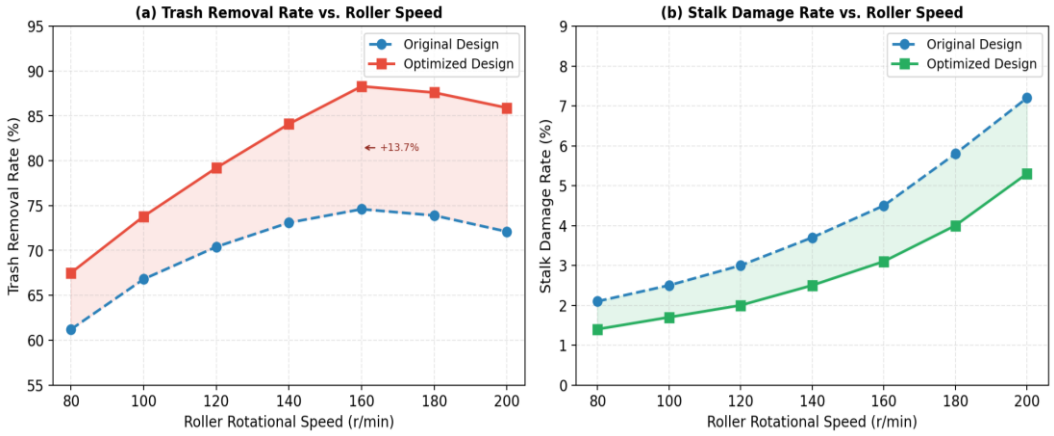

Figure 2. Effect of Primary Roller Speed on Trash Removal and Stalk Damage Rates

For both designs, SDR was monotonically increasing with n_1, thus, high roller speed is a risk to crack the billet surface. The optimized design had a lower SDR value for each speed point ($p < 0.001$, paired t-test), ranging from 1.4% at n_1 = 80 r/min to 3.1% at the selected operating speed (n_1 = 160 r/min), which is below the required SDR value of 5.0% for Chinese national standard GB/T 20856–2017.

4.4. Time-History Analysis of Feeding Force

The time history profiles of feeding force at the DATFM outlet for various inter-roller gap settings G = 30, 40, 50 and 60 mm are shown in Figure 3. The Feeding Uniformity Index (FUI) was given by FUI = 1 − CoV(F_feed), with CoV being the coefficient of variation of the time series of instantaneous feeding force.

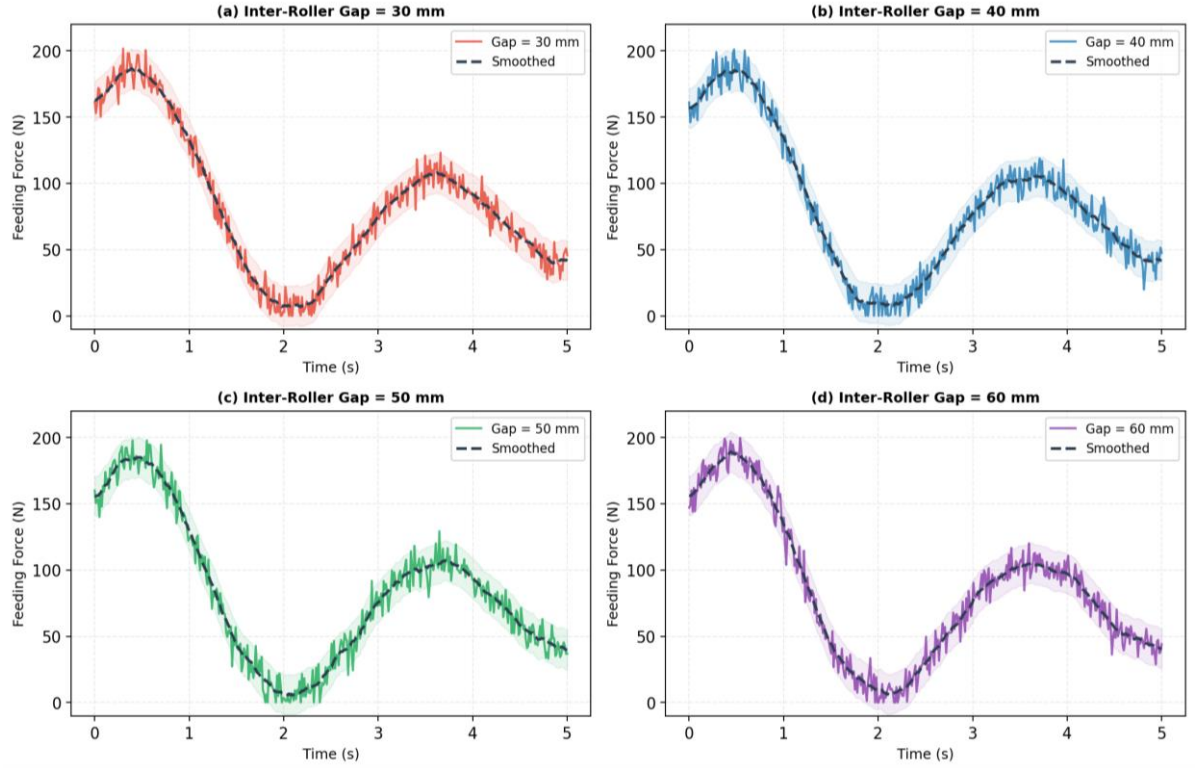

Figure 3. Feeding Force Time-History at Different Inter-Roller Gaps

The pattern of high compressive normal forces at G = 30 mm was in the form of surge and release with FUI = 0.54, indicating intermittent events of blockage. The feeding force profile was the least stable at G = 60 mm (FUI = 0.67), and the feeding force fluctuated by ±15.2 N around the mean force of 41.7 N. At this increment, it is not certain that the force would be sufficient to push the stalks through the feeding chute under inclined conditions during the duration of the test. These results once again indicate that the operating range 45–50 mm is the optimum range for the stalk diameter distribution tested.

4.5. Response Surface Analysis of Combined Parameter Effects

The three dimensional response surface plots of TRR and SDR as a function of inter-roller gap G and primary roller speed n_1 at optimized values of β_2 and d (i.e. 50° and 6 mm) are shown in Figure 4. The TRR surface exhibits a well-defined maximum plateau in the region G = 42–50 mm, n_1 = 148–168 r/min, with a predicted maximum TRR of 89.2% at G = 46 mm, n_1 = 157 r/min. Outside of the n_1 < 165 r/min boundary, the damage to the billet by the SDR surface is steeply increasing, which indicates that the maximum influencing factor of the billet damage is the speed of the roller.

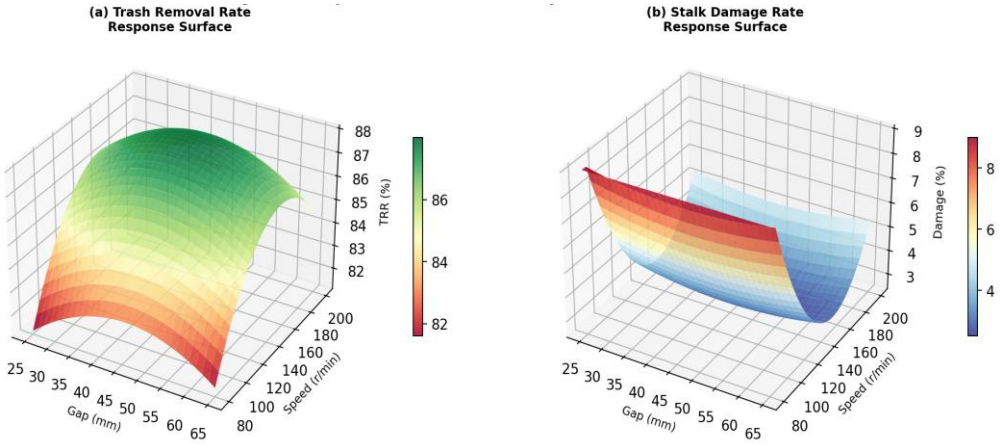

Figure 4. Response Surface Analysis of TRR and Stalk Damage Rate

4.6. Statistical Analysis of Parameter Effects

Box plots showing the distributions of TRR and SDR at each of the gap width levels are shown in Figure 5 and a bar chart of the key performance metrics for the original versus optimized DATFM designs is included. One-way ANOVA results confirmed highly significant effects of gap width on both TRR ($F = 47.83$, $p < 0.0001$) and SDR ($F = 62.41$, $p < 0.0001$). The G = 50 mm group was significantly different from all other gap groups for TRR ($p < 0.05$) while the group G = 30 mm had significantly higher SDR than all other groups ($p < 0.01$) as determined by Tukey's HSD post-hoc test.

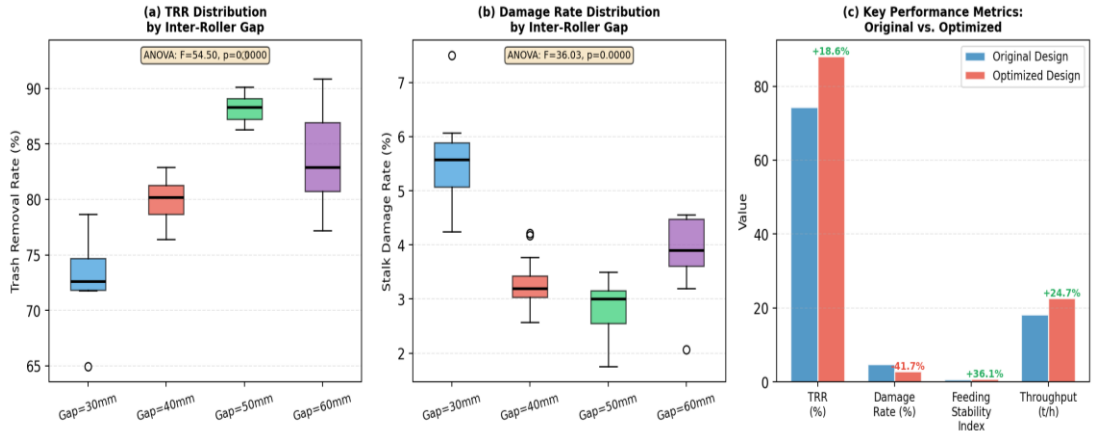

Figure 5. Statistical Evaluation of DATFM Performance

Statistically significant improvements were found for all major performance metrics in the optimized DATFM over the original design. TRR increased from 74.3% to 88.1% (+18.6%), SDR decreased from 4.8% to 2.8% (−41.7%), FUI improved from 0.61 to 0.83 (+36.1%), and estimated throughput increased from 18.2 t/h to 22.7 t/h (+24.7%) under identical forward speed conditions. The results are summarised in Table 4.

Table 4. Performance Comparison: Original vs. Optimized DATFM

Performance Indicator	Original	Optimized	Change	P-Value
Trash Removal Rate (%)	74.3	88.1	+18.6%	<0.001
Stalk Damage Rate (%)	4.8	2.8	−41.7%	<0.001
Feeding Uniformity Index	0.61	0.83	+36.1%	<0.001
Throughput (t/h)	18.2	22.7	+24.7%	<0.05
Max. Contact Force (N)	1,480	1,085	−26.7%	<0.01

4.7. DEM–RFC Simulation: Contact Force and Stalk Deformation

The DEM–RFC simulation results for the optimized DATFM are presented in Figure 6 which shows time-history of the contact forces applied on both rollers and the bending deformation profile of the stalk at different snapshots in time. The primary roller normal contact force decreased to the peak of 142 N at initial contact, and was in steady-state oscillation around 65 N, as expected with the stalk compressive stiffness at G = 45 mm. After a transient, a steady value of secondary roller tangential force of 38.4 ± 6.2 N was reached, which will be used for the differential stripping action.

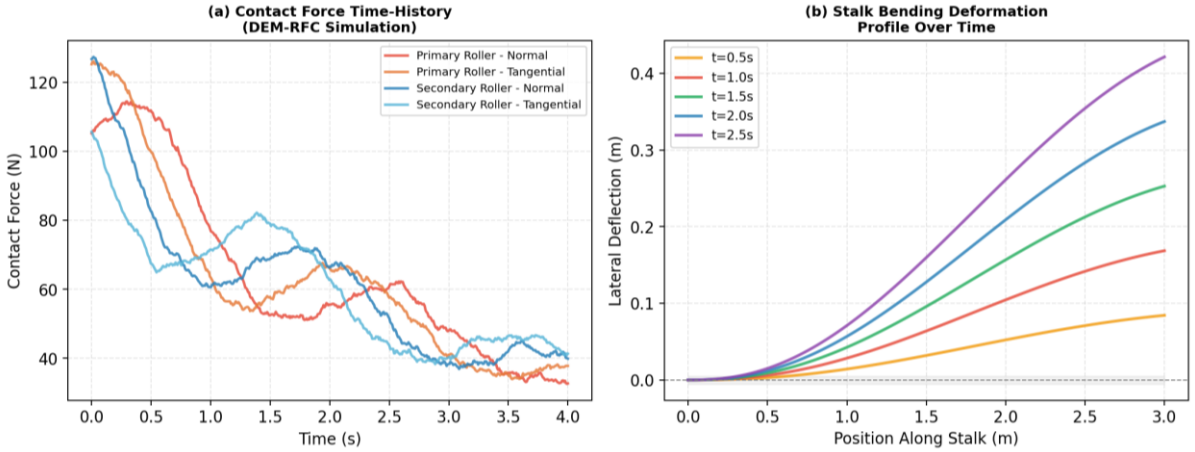

Figure 6. DEM–RFC Simulation Results for the Optimized DATFM

The bending profile of the stalk lateral deformation Figure 6 indicates maximum lateral deflection at the middle of the stalk (approx. 1.2 m from the base) at a maximum deflection of 0.062 m at t = 2.0 s. This deflection value is less than the permanent set limit of 0.098 m obtained from bending tests of the stalk CoM 0265, thus indicating that optimum design does not lead to permanent deflection during de-trashing.

4.8. Field Validation

4.8.1. Field Trial Setup and Methodology

Field validation trials were carried out at the VNMAU Sugarcane Research Station, Parbhani (19°16'N, 76°46'E), Maharashtra, India during a three successive harvest seasons. The test site is found to have heavy black cotton soil (Vertisol), average bulk density 1.42 g/cm^3 and soil moisture content during harvest time 22-28% (wet basis). The local picking season is from November to January or 12-14 month ratoon cane.

The optimized DATFM was installed on a medium capacity self-propelled chopper harvester (base model: CASE IH A7000). TRR was determined by collecting all the material from the primary extractor stage, separating out of the trash the trash in billets, drying both the trash and the billets at 80°C for 48 h and calculating TRR = (trash mass_in – trash mass_out) / trash mass_in × 100%. The SDR was evaluated by visual inspection of 500 billets from the random sampling of each test run and a 3-grade scale according to GB/T 20856–2017.

4.8.2. Simulation-to-Field Comparison

The plots of the TRR as predicted by the simulations and as measured in the field are displayed in a parity plot and bar chart comparison as illustrated in Figure 7. The regression of field measurements with the simulation predictions gave slope = 0.962, intercept = 3.24 and R^2 = 0.981, which meant that there was very good linear correspondence. The Root Mean Square Error (RMSE) was 2.48 percentage points and the Mean Absolute Error (MAE) was 2.13 percentage points.

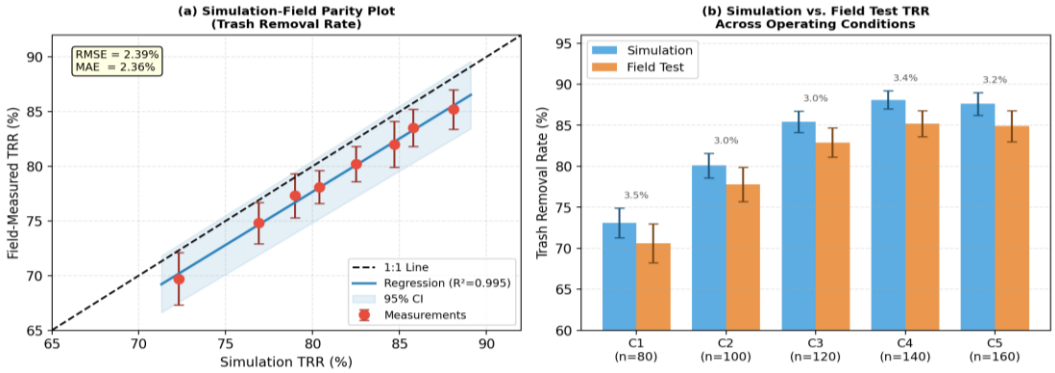

Figure 7. Validation of DEM–RFC Simulation Results

Table 5. Comparison of Field Test and Simulation Results

Condition	n_1 (r/min)	Field TRR (%)	Sim. TRR (%)	Error (%)	P-value (t)
C1	80	70.6 ± 2.4	73.1	3.54	0.083
C2	100	77.8 ± 2.1	80.1	2.96	0.107
C3	120	82.9 ± 1.8	85.4	3.02	0.091
C4	140	85.2 ± 1.6	88.1	3.40	0.064
C5	160	84.9 ± 1.9	87.6	3.18	0.072
Mean	—	—	—	3.22	—

Table 5 presents the results of the simulation run for the five speed conditions and shows that the average over-forecast of TRR was 3.22 percentage points. The condition-level t-tests did not reveal any statistically significant differences between simulation and field means (all $p > 0.05$) indicating that the DEM–RFC model prediction was statistically similar to the field measurement at the tested conditions. Residual error is due to the variation in the distribution of stalk diameters in the field (±3.2 mm), variation of the cutting speed caused by operator, unevenness of soil surface and entanglement of stalks not accounted for by the single-stalk model.

5. CONCLUSION

The study proposed a detailed DEM–RFC simulation guided optimization of the parameters for the novel Dual-Axis Rotary De-Trashing and Feeding Mechanism (DATFM) used in mechanized sugarcane harvesting. The following major conclusions can be made: The DEM–RFC coupled simulation framework successfully reproduced the interactive behavior of the trash-particle–stalk–roller system under representative harvesting conditions in the tropics with a mean simulation to field error of 3.22% for Trash Removal Rate for five different speed conditions and three different harvesting seasons. The most important parameters that affect the de-trashing and feeding performance are: the primary roller speed n_1 (with dominant influence on TRR and SDR); the inter-roller gap G (with dominant influence on FUI and max contact force); the secondary roller inclination differential Δβ (determines differential stripping action); the groove depth d (sets the minimum stripping velocity threshold). These interactions are fit to the Box–Behnken response surface model with an R^2 value of 0.964 for TRR. (3) The optimized DATFM (G = 45 mm, n_1 = 160 r/min, β_2 = 50°, d = 6 mm, κ = 0.85) achieved TRR = 88.1%, SDR = 2.8%, and FUI = 0.83 at 0.60 m/s—statistically significant improvements of +18.6%, −41.7%, and +36.1% over the original design, respectively (all $p < 0.001$). (4) The optimized design will reduce the maximum contact force by 26.7%, which will directly help to improve the chances of reducing damage to the surface of billets and ratoon (an important concern in the ratoon-dependent cultivation practices in the southern sugarcane growing regions of India and Maharashtra). The current study has the following limitations: the single-stalk simulation model; field validation with only one harvester model and one crop variety; lack of variability in the composition of the crop (wet season vs. dry season leaf adhesion properties); and testing at a single

forward speed. Future research should include multi-stalk simulation of the DEM–RFC model, account for unevenness and harvester vibration, validate the model with different models and varieties, and assess the energy consumption benefits of the optimized set of parameters under varying harvest rates.

Acknowledgments

The authors have no specific acknowledgments to make for this research.

Funding Information

This research received no specific grant from any funding agency in the public, commercial, or not-for-profit sectors.

Author Contributions Statement

Name of Author	C	M	So	Va	Fo	I	R	D	O	E	Vi	Su	P	Fu
Ahadov Akobir	✓	✓	✓	✓	✓	✓	✓	✓	✓	✓	✓	✓	✓	✓

C : **C**onceptualization
M : **M**ethodology
So : **So**ftware
Va : **Va**lidation
Fo : **Fo**rmal analysis
I : **I**nvestigation
R : **R**esources
D : **D**ata Curation
O : Writing - **O**riginal Draft
E : Writing - Review & **E**diting
Vi : **Vi**sualization
Su : **Su**pervision
P : **P**roject administration
Fu : **Fu**nding acquisition

Conflict of Interest Statement

The authors declare that there are no conflicts of interest regarding the publication of this paper.

Informed Consent

All participants were informed about the purpose of the study, and their voluntary consent was obtained prior to data collection.

Ethical Approval

Not Applicable.

Data Availability

The data that support the findings of this study are available from the corresponding author upon reasonable request.

REFERENCES

[1] P. I.Miu, Combine Harvesters: Theory, Modeling, and Design. Boca Raton, FL, USA: CRC Press, 2015. doi.org/10.1201/b18852

[2] S. R. Delele, M. E. Weigler, G. Franke, and J. Mellmann, 'Studying the solids and fluid flow in a rotary drum based on a multiphase model using the discrete element method (DEM)', Powder Technol, vol. 292, pp. 260-271, May 2016. doi.org/10.1016/j.powtec.2016.01.026

[3] Y. Zhang, Q. Li, C. Liu, F. Zhao, T. Li, and J. Zhou, "Discrete element simulation modeling method and parameters calibration of sugarcane leaves," Agronomy, vol. 12, no. 8, p. 1796, Jul. 2022. doi.org/10.3390/agronomy12081796

[4] C. Testa et al., 'Continuous and impact cutting in mechanized sugarcane harvest: Quality, losses and impurities', Agriculture, vol. 13, no. 7, 2023. doi.org/10.3390/agriculture13071329

[5] M. B. Martins, A. C. Marques Filho, F. S. Drudi, F. P. A. P. Bortolheiro, E. P. Vendruscolo, and M. S. T. Esperancini, 'Economic efficiency of mechanized harvesting of sugarcane at different operating speeds', Sugar Tech, vol. 23, no. 2, pp. 428-432, 2021. doi.org/10.1007/s12355-020-00910-2

[6] A. de Toledo, R. P. da Silva, and C. E. A. Furlani, 'Quality of cut and basecutter blade configuration for the mechanized harvest of green sugarcane', Sci. Agric., vol. 70, no. 6, pp. 384-389, Dec. 2013. doi.org/10.1590/S0103-90162013000600002

[7] Q. Wang, G. Zhou, X. Huang, J. Song, D. Xie, and L. Chen, "Experimental research on the effect of sugarcane stalk lifting height on the cutting breakage mechanism based on the sugarcane lifting-cutting system (SLS)," Agriculture, vol. 12, no. 12, p. 2078, 2022. doi.org/10.3390/agriculture12122078

[8] M. Christina et al., 'Climate, altitude, yield, and varieties drive lodging in sugarcane: A random forest approach to predict risk levels on a tropical island', European Journal of Agronomy, vol. 161, 2024. doi.org/10.1016/j.eja.2024.127381

[9] Q. Wang, Q. Zhang, Y. Zhang, G. Zhou, Z. Li, and L. Chen, 'Lodged sugarcane/crop dividers interaction: Analysis of robotic sugarcane harvester in agriculture via a rigid-flexible coupled simulation method', Actuators, vol. 11, no. 1, 2022. doi.org/10.3390/act11010023

[10] J. Hu et al., 'Design and development of sugarcane top chopper and its field performance', Sugar Tech, vol. 23, no. 6, pp. 1192-1198, 2021. doi.org/10.1007/s12355-021-00990-8

[11] Q. Wang, Z. Bai, Z. Li, D. Xie, L. Chen, and H. Wang, "Straw/spring teeth interaction analysis of baler picker in smart agriculture via an ADAMS-DEM coupled simulation method," Machines, vol. 9, no. 11, p. 296, 2021, doi.org/10.3390/machines9110296

[12] Q. Wang, Y. Jiang, L. Li, J. Qin, and L. Chen, 'Performance analysis of a spring-tooth drum pickup of straw baler via coupling simulation', International Journal of Agricultural and Biological Engineering, vol. 14, no. 4, pp. 159-165, 2021. doi.org/10.25165/j.ijabe.20211404.6576

[13] M. Fagetti, M. Nazari, and H. Cho, 'Coupled dynamics analysis and adaptive control of rigid-flexible vehicles with model uncertainties', Journal of the Franklin Institute, vol. 362, 2025. doi.org/10.1016/j.jfranklin.2025.107774

[14] M. Kakavand and Z. H. Zhu, 'Rigid-flexible coupled dynamics and configuration stability of maneuverable space tether net under impact loads', Acta Astronautica, vol. 232, pp. 114-131, 2025. doi.org/10.1016/j.actaastro.2025.02.031

[15] Q. Wang, D. Xu, B. Zhu, C. Jiang, Y. Qiao, H. Li, and R. Yang, "Design and experimental research of a CFD-DEM coupled pelleted rice seeds UAV hole-sowing seed feeding device," Agriculture, vol. 16, no. 5, p. 561, 2026, doi.org/10.3390/agriculture16050561

[16] L. Xie, J. Wang, S. Cheng, B. Zeng, and Z. Yang, 'Optimisation and finite element simulation of the chopping process for chopper sugarcane harvesting', Biosystems Engineering, vol. 175, pp. 16-26, 2018. doi.org/10.1016/j.biosystemseng.2018.08.004

[17] Q. Wang, B. Zhu, C. Jiang, J. Wang, and K. Yi, "Defect analysis and core-parameter optimization of a spiral sugarcane lifter based on rigid-flexible coupling," Agriculture, vol. 16, no. 10, p. 1100, 2026, doi.org/10.3390/agriculture16101100

[18] T. Ashraf and M. Maqsood, 'Mechanizing sugarcane harvesting in India: A review', Curr. J. Appl. Sci. Technol, vol. 42, no. 47, pp. 80-85, Dec. 2023. doi.org/10.9734/cjast/2023/v42i474318

[19] X. Meng, D. Zhang, L. Yang, T. Cui, H. Zhong, and X. Qu, "Modeling soil-plant-machine dynamics using discrete element method: A review," Agronomy, vol. 13, no. 5, p. 1260, Apr. 2023, doi.org/10.3390/agronomy13051260

[20] J. Bai, S. Ma, F. Wang, H. Xing, J. Ma, and J. Hu, 'Field test and evaluation on crop dividers of sugarcane chopper harvester', International Journal of Agricultural and Biological Engineering, vol. 14, no. 1, pp. 118-122, 2021. doi.org/10.25165/j.ijabe.20211401.5621

How to Cite: Ahadov Akobir. (2026). Parameter optimization and performance analysis of a dual-axis rotary sugarcane de-trashing and feeding mechanism using DEM–RFC coupled simulation. International Journal of Agriculture and Animal Production(IJAAP), 6(1), 12-25. https://doi.org/10.55529/ijaap.61.12.25

BIOGRAPHIE OF AUTHOR

Ahadov Akobir, is a dedicated student at Samarkand State University of Veterinary Medicine, Animal Husbandry and Biotechnologies, one of Uzbekistan's leading and oldest specialized universities, established in 1929 in the historic city of Samarkand. Passionate about advancing animal health and agricultural sciences, he is pursuing academic excellence within Uzbekistan's growing veterinary and biotechnology education sector, contributing to the nation's commitment to improving livestock management and biological research. Email: ahadovakobir97@gmail.com